Journal of Cultural Heritage 72 (2025) 13–23

Contents lists available at ScienceDirect

Journal of Cultural Heritage

journal homepage: www.elsevier.com/locate/culher

VSI: TECHNART 2023 selected papers

The "Black Panther": A multi-analytical study on the statue of the football player Eusébio da Silva Ferreira

Ana Catarina Pinheiro[a,b,c,*], Mathilda Larsson Coutinho[a,b], Carlo Bottaini[a,b,d], Marius Araújo[e], Vera Pires[a,b], Bárbara Campos Maia[f], Joana Madureira[f], Filipa Pereira[f]

[a] Laboratório HERCULES, Universidade de Évora, Largo Marquês de Marialva, 8, 7000-809 Évora, Portugal
[b] IN2PAST, Laboratório Associado, Universidade de Évora, Évora, Portugal
[c] Laboratório José de Figueiredo, MMP-EPE, Rua das Janelas Verdes s/n 1249-018 Lisboa, Portugal
[d] Geography, Archaeology and Palaeoecology, School of Natural and Built Environment, Queen's University Belfast, Elmwood Building, Belfast BT7 1NN, Northern Ireland, UK
[e] Arteria Lab, Universidade de Évora, Centro Magallanes Indústrias Culturais e Criativas, Colégio dos Leões - Universidade de Évora, Estrada dos Leões, 38, 7005-208 Évora, Portugal
[f] Direção de Património Cultural do Sport Lisboa e Benfica, Estádio do Sport Lisboa e Benfica, Avenida Eusébio da Silva Ferreira, 1500-313 Lisboa, Portugal

ARTICLE INFO

Article history:
Received 4 November 2023
Accepted 28 December 2024

Keywords:
Metal statue
Conservation
Alloy
Copper
Corrosion
Analytical techniques

ABSTRACT

The iconic Eusébio da Silva Ferreira statue attracts a lot of attention from Sport Lisboa e Benfica Football fans and fans worldwide who, eager to show their affection and respect for the player, touch and pose with the statue, a proximity that the sports Club promotes and encourages. The statue (classified as a bronze but the alloy was not known) is in a good state of conservation but localised signs of possible corrosion – visible green/blue, orange and white stains - appear intermittently and an alteration to the original position of the statue leaves a cloud of uncertainty when it comes to its physical stability. To address these questions a multi-analytical combined approach was devised with the use of portable equipment (digital microscope, h-XRF, 3D scanner and a Pundit PL-200) and laboratory techniques (µXRD, µRaman and VP-SEM-EDS). Contrary to what was previously thought, the sculpture was produced using a ternary Cu–Sn–Zn alloy rich in Pb. The coloured deposits analysed revealed the presence of Cu, Fe and Zn which translates into active corrosion that needs to be closely monitored. Other deposits are due to atmospheric debris. Copper phthalocyanine, a blue-green pigment was identified which may be related to the patina. The ultrasound technique has allowed the determination of the relative thickness of the statue but fell short of determining the actual position of a sustaining inner rod. Further studies are needed to address this issue.

1. Introduction

Sports activities are transversal to human culture. The recognition of sports as part of our society elicits the awareness of the cultural value of the sport-related cultural heritage. Ever since its foundation, in 1904, Sport Lisboa e Benfica has produced and reunited a large heritage collection. In this regard, the Storage, Conservation and Restoration Department and the Documentation and Information Centre, were created in 2010 for the preservation, management, investigation and communication of the Club's cultural heritage collection. Aware that the preservation of its cultural and heritage collection equals the preservation of the Club's identity, the Club inaugurated the Benfica Museum - Cosme Damião in 2013 and established, in 2015, the Cultural Heritage Direction whose mission is to preserve, valorise and communicate this heritage through its conservation, research, interpretation and communication, as well as through other educational and cultural programmes.

One of Benfica's most prized icons is the outdoor statue of Eusébio da Silva Ferreira (Fig. 1) which attracts the attention of (football) fans worldwide.

The public is eager to show its affection and respect for the player, and what it represents, and they do so by touching and posing with the statue, a proximity that the Sport Lisboa e Benfica Club promotes and encourages, unlike most public artworks. Produced in 1992, the statue is in a superficial good state of conserva-

* Corresponding author at: Laboratório HERCULES, Universidade de Évora, Largo Marquês de Marialva, 8, 7000-809 Évora, Portugal.
E-mail address: acmsp@uevora.pt (A.C. Pinheiro).

https://doi.org/10.1016/j.culher.2024.12.026

Fig. 1. Eusébio da Silva Ferreira Statue, located at Praça Centenário at Sport Lisboa e Benfica stadium. The statue's right hand is frequently touched by fans and clearly shows the effects of this action (adapted from a photograph by João Freitas).

tion as is expected from its recent production date but exposure to pollution [1], atmospheric conditions [2–5] and human interaction has begun to take its toll.

The patina is wearing off in the most touched areas (Fig. 1), as a consequence of the public interaction and there are localised signs of possible corrosion products with green/blue, orange and white colouration visible in specific locations (Fig. 2a and b, Fig. 5).

The atmospheric corrosion of copper alloys caused by the physicochemical reactions between the metal and environment has been extensively studied [1,4,5]. The potential discoloration of the surface due to corrosion is one of the earliest visible signs of outdoor exposure, resulting from the formation of oxides, carbonates, or sulphates as metal ions leach from the sculpture [1,3–6].

Although the statue has been catalogued as a bronze, the exact composition of the alloy used for its production was unknown. In an interview, the artist mentioned requesting a bronze alloy for the statue casting but left the exact alloy composition decision to the foundry company that eventually assembled his design. Neither is the patination process used for the sculpture known. This company is now closed for business and therefore unable to provide any information.

Adding to the possible corrosion products observed and unknown alloy composition (relevant to discerning the best possible conservation treatments going forward and fully understanding the corrosion patterns), the statue may also be suffering from mechanical stress caused by a shift from its original position in the old Sport Lisboa e Benfica stadium. Designed to be displayed in a predetermined state of equilibrium, with Eusébio in a kicking position, the statue was first installed at the former Estádio da Luz, which met its demise in 2003. The statue then found a new home at the entrance to the new stadium in 2002, only to be moved again in 2008 to its current location at Praça Centenário within the modern stadium complex. These relocations have resulted in a noticeable change in the player's posture, now reclining, and a shift in the direction of his gaze, no longer fixed on the ball, as shown in Fig. 3a, b and c.

Another request from the artist to the foundry company was the insertion of a supporting stainless-steel rod structure inside the left leg from the foot to the hip. Assuming that this rod was placed as requested, it is the only support point to the ground. The current state of conservation or possible position shift of the rod is unknown. Given the intense interaction of the statue with the visiting public (constant posing for photographs, touching, sitting) this is of particular concern for the Storage, Conservation and Restoration Department of Sport Lisboa e Benfica [7].

The statue of Eusébio da Silva Ferreira has become a fundamental and precious icon of Benfica history and mysticism, a "mandatory" crossing and stopping point for all Benfica fans and tourists visiting the Sport Lisboa e Benfica stadium. The Club, and its conservation team, face a challenge: the material and structural preservation of the statue (and its safety) vs the promotion of a close contact with the public as part of the social value of the statue.

The preservation of metallic cultural artefacts when exposed to outdoor elements is an exceedingly critical concern, often undervalued in its intricacy and inadequately tackled. Urban settings serve as notably severe case studies due to the exacerbation of weathering effects by pollution and the existence of corrosive compounds in the air demanding a meticulous examination of the mechanisms causing degradation in metallic cultural heritage [1,6,8].

Analytical techniques play a crucial role in the preservation, restoration, and study of statues. To ensure the longevity and historical significance of these important artefacts, various analytical methods are employed. Non-destructive techniques like X-ray

Fig. 2. a and b- The left leg presents greenish-blue deposits, and the right foot has developed rounded orange ones. See Fig. 4 for their locations (B and I, respectively). (For interpretation of the references to color in this figure legend, the reader is referred to the web version of this article.)

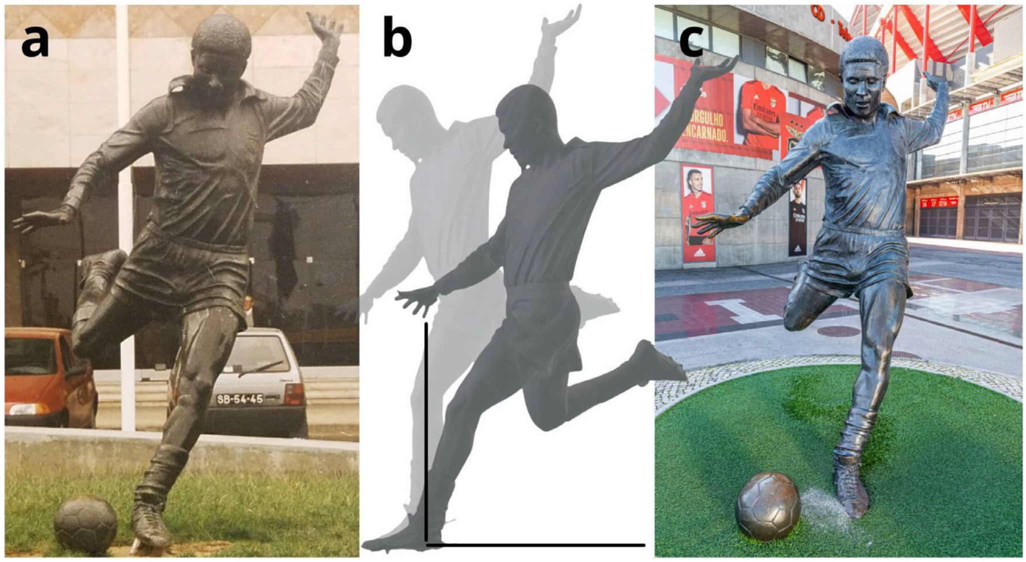

Fig. 3. a) Photography of the statue in the original position, determined by the artist in the former Sport Lisboa e Benfica stadium (reference: Artist Duker Bower); c) photography of the statue in the current location in the new Sport Lisboa e Benfica stadium (author of the photography: João Freitas); b) Between the two photographs, a composition depicting the original (light grey) and the current (dark grey) position of the statue. This schematic representation was obtained from the 3D model of the statue. (For interpretation of the references to color in this figure legend, the reader is referred to the web version of this article.)

fluorescence spectroscopy (XRF) are used to determine the elemental composition of the metallic alloys. Microscopic analysis, such as scanning electron microscopy (SEM-EDS), micro X-Ray Diffraction (μXRD) and micro Raman (μRaman), can provide insights into the metal microstructure and the distribution and characterization of corrosion products, assisting in the precise conservation approach for these valuable cultural artefacts. By employing these analytical techniques, experts gain a better understanding of the metallic alloy and corrosion processes affecting metal statues, thereby enabling more accurate preservation efforts that will endure for generations to come.

Research aims: To address critical conservation questions and formulate effective conservation strategies, a comprehensive, multi-analytical approach was developed, combining both portable and laboratory-based equipment. Additionally, to enhance visualisation and monitoring of corrosion issues, a high-definition 3D model of the statue was created.

2. Materials and methods

2.1. Eusébio's sculpture

The Eusébio da Silva Ferreira statue currently located at Praça Centenário in Sport Lisboa e Benfica stadium (Lisbon) was produced by the American sculptor, Duker Bower, commissioned by Vitor Batista, a Portuguese member and an enthusiastic supporter of the Club. It is a realistic representation of young Eusébio da Silva Ferreira, also known as "Black Panther", a worldwide famous football player, depicted while preparing to kick the ball. The statue was offered to the Club and inaugurated on January 25, 1992, coinciding with the 50th anniversary of Eusébio. The statue is 2,25 m high, 1,88 m wide and weighs approximately 400 kg. The manufacturing method used was lost wax casting production. It is assumed that the statue was cast in several different parts as it is possible to distinguish the welded joint areas between the torso and legs. However, the exact number of parts remains unknown.

The statue is localized in an intense traffic area of Lisbon (Latitude: 38° 45′ 5.77″ N. Longitude: −9° 11′ 2.91″ W) [9] and the lack of protection from atmospheric conditions [10] must be taken into consideration when interpreting data resulting from the deposits encountered.

2.2. Analytical approach

In this study, we have adopted a multi-analytical approach to address the unique challenges of conserving the statue of Eusébio. The techniques and equipment used are associated with the problem being addressed and the approach taken was the least invasive possible, as defined by the ECCO guidelines for conservation of cultural heritage [11].

By integrating different analytical techniques, we aim to gain a comprehensive understanding of the statue's composition, surface characteristics and relevant conservation issues. This approach will allow us to define a science-based strategy for the conservation of the statue that will enable it to continue to interact with football fans.

2.2.1. Digital microscopy

A digital microscope (Pancellent, Inskam software) was used to evaluate the surface of the studied statue, ease sampling and record macro images.

2.2.2. X-ray fluorescence chemical characterization of the alloy and patina

To determine the elemental composition of the bulk metal and the patinated surface, a portable handheld equipment (h-XRF) Tracer 5i Bruker (AXS Karlsruhe, Germany), with a Be window and a 50 kV, 4 W, Rh X-ray tube source and a Silicon Drift Detector with a resolution of <140 eV at 250,000 cps at the Mn Kα line was used. Analysis was performed using the Bruker built-in Ancient Copper Alloys Calibration program. The spectra were acquired using the Bruker ARTAX v.8.0.0.476 software. Each point was analysed in three spots (8 mm spot size) for 60s.

The XRF analyses were conducted without the prior removal of the corrosion layers covering the sculpture. To determine the composition of the bulk metal, we targeted areas that had been worn down due to frequent touch by Eusébio's admirers and fans, where

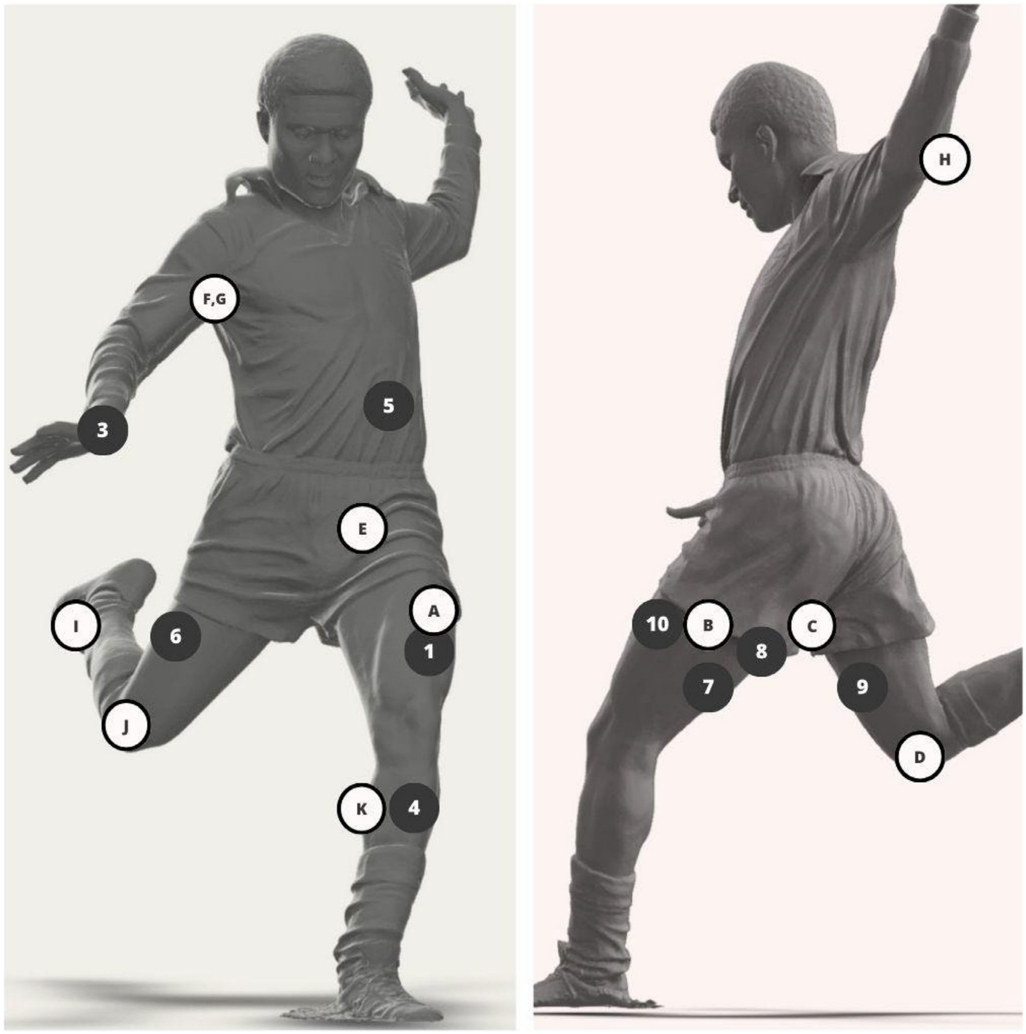

Fig. 4. 3D model of the statue of Eusebio da Silva Ferreira. The numbers (1–10) correspond to the locations where the h-XRF was used. Sample number 2 was taken on the football surface, not represented here. The letters (A-K) represent the location where micro-samples were removed for observation under XRD and SEM-EDS (see 2.2.3 and 2.2.4.). Locations A and I refer also to image 2a and 2b, respectively.

the patina was visually absent, providing better access to the underlying alloy (as shown in Fig. 1). Additionally, analyses were performed on regions with dark patina to gather information on the patinated surface. The numbers (1 to 10) in Fig. 4 indicate the locations where this methodology was applied.

2.2.3. X-ray diffraction characterisation of coloured surface deposits

Micro samples of surface deposits and corrosion products were collected on-site, taken with a scalpel and transported in an Eppendorf to be analysed in the laboratory. To determine the mineralogical composition samples were analysed with an XRD Bruker D8 Discover diffractometer (with CuKα radiation) operating in microanalysis mode carried out at 40 kV and 40 mA and the measurements were made between the 5° and the 75° 2θ, a step of 1.0° and 1 s per step. EVA software (with ICDD PDF X-ray patterns database) was used for the identification of the mineral phases. To determine their microstructure and morphology some of the samples were analysed with variable pressure-scanning electron microscope with an energy dispersive X-ray spectrometer (VP-SEM-EDS). Analysis was carried out with a Hitachi 3700 N scanning electron microscope interfaced with a Bruker AXS XFlashVR Silicon Drift Detector (129 eV of spectral resolution at FWHM - Mn Ka). The operating conditions for EDS analysis were 20 kV of accelerating voltage, 10 mm of working distance and 120 mA of emission current.

2.2.4. μ - Raman characterisation of coloured surface deposits

Micro-Raman spectroscopy (μ-RS) was used on surface deposits collected from the sculpture with a Raman spectrometer Horiba XPlora equipped with a diode laser of 10.3 mW operating at 785 nm, coupled to an Olympus microscope. Raman spectra were acquired in extended mode in the 100–1500 cm^{-1} region. The laser was focused with an Olympus 50× or 100× lens, 10 % of the laser power on the sample surface (5s exposure, 5 cycles of accumulation). The spectra were analysed with the equipment software (LabSPEC 5 from Horiba Jobin Yvon, France).

2.2.5. Ultrasonic testing to evaluate the statue stability

As happens in medicine, ultrasounds can be employed to determine the thickness of a sculpture [5]. The sounds produced in any environment are reflected or reverberate off the walls that make up that environment and can also be transmitted. This phenomenon is the foundation of ultrasonic testing of materials. Just as a sound wave reflects when it strikes a surface, the vibration or ultrasonic wave also reflects when it travels through an elastic medium; similarly, the vibration or ultrasonic wave will reflect

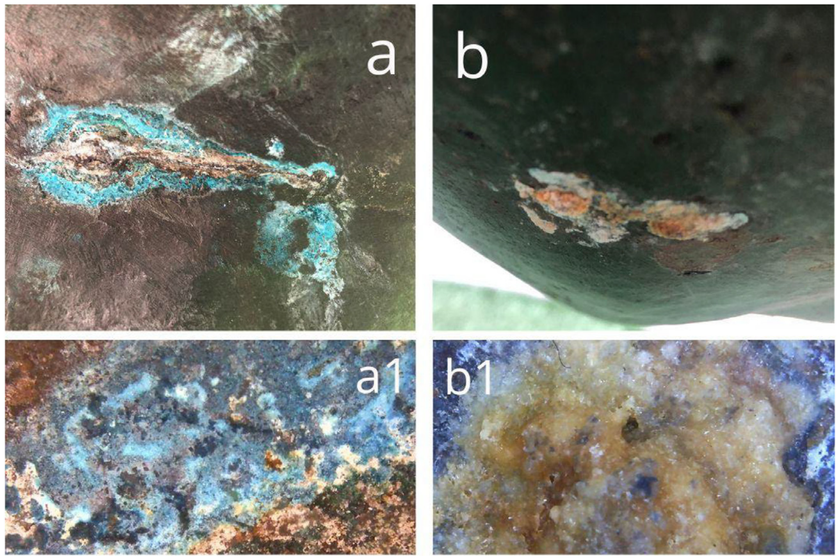

Fig. 5. a and b) Coloured deposits on location B and D, respectively (see Fig. 4); a1 and b1) Expanded view (magnification 12x) of the deposits using a portable microscope. (For interpretation of the references to color in this figure legend, the reader is referred to the web version of this article.)

when it strikes a discontinuity or internal flaw in the medium considered. Using specific equipment, it is possible to detect the reflections coming from inside the examined part, localising and interpreting the discontinuities.

In order to determine the structural/physical stability of the statue, it was very important to determine the conservation conditions of the left leg and confirm 1) the existence of a stainless rod structure and 2) the condition of this supporting element, supposedly extending from the foot to the hip. Since ultrasounds can penetrate metal, deliver results on the surface discontinuities and configure a non-invasive approach, a Ultrasonic Pulse Echo testing equipment Pundit PL-200 – PROCEQ with 54 Hz conic transducers was used in this particular case to assess the transmission time and, from the obtained results, attempt to determine the thickness of the statue at point of measurement and, by comparison, determine where the rod would be positioned.

2.2.6. Structured-light 3D scanning model

3D scans of the Eusébio Statue were carried out by _ARTERIA_LAB. The acquisition was done at the location, outdoors, under indirect sunlight, and at dusk to avoid reflections. An Artec Eva 3D Scanner was used for larger areas and an Artec Spider for sharper detail acquisition in smaller areas. Scans were performed in parallel patterns at approximately 0.2–1 m from the surfaces, keeping the scanner parallel to the surface and trying to cover the complete area of interest. The laptop used for all scans was a MSI Raider series gaming laptop, with an Intel core i7-8750h CPU @ 2.2 GHz, 32Gb of RAM and a Nvidia Geforce RTX graphics card. Post-processing was performed on the same equipment, on Artec Studio 16 Professional software.

3. Results and discussion

3.1. Digital microscopy

A digital microscope is a valuable tool to better visualize and understand the morphology of the coloured deposits. Fig. 5a refers to location B and Fig. 5b to location D in Fig. 4. Fig. 5 a1 and b1 refer to the enlarged versions of these locations and these help in the process of sample retrieval. These deposits exhibit green, orange and white hues. The composition of these hues was later investigated through analytical methods.

3.2. Composition of the alloy

The h-XRF results from various points across both free-patina areas and patinated surfaces are shown in Table 1. The analysed points were previously presented in Fig. 4.

Considering the statue's exposure to atmospheric conditions, pollution, and human interaction, it's reasonable to assume that results, particularly those achieved on the patinated surface, may slightly differ from the original alloy [12,13]. However, since it was not feasible to remove surface metal or obtain drill core samples, the objective of the h-XRF analysis was to determine the elemental composition of the original alloy as accurately as possible, despite the limitations inherent to surface corrosion products.

The results reveal that the bulk metal is composed of copper (Cu), ranging from 69.15 % (Point 4) to 81.42 % (Point 9), with significant but variable levels of zinc (Zn) (from 0.43 % at Point 9 to 24.37 % at Point 1) and tin (Sn) (from 3.87 % at Point 1 to 14.05 % at Point 9). Lead (Pb) concentrations range between 1.92 % (Point 3) and 5.06 % (Point 8). The alloy of the sculpture, consistent with a Cu–Sn–Zn alloy rich in lead that also contains minor elements such as iron (Fe), ranging from 0.31 % (Point 1) to 1.62 % (Point 7), nickel (Ni) up to 0.26 % (Point 2), and arsenic (As) up to 0.07 % (Point 4).

For the major elements, significant variations were observed across the analysed points. Notably, Zn displayed considerable variability, particularly in the patinated areas, where two points—Points 6 and 9—recorded levels below 10 %. Due to the non-destructive and surface-based methodology employed in this study, we cannot definitively confirm that these variations represent the actual composition of the alloy. Instead, it is more plausible that, in specific regions, these findings reflect a process of Zn depletion resulting from prolonged environmental exposure (Fig. 6A), particularly if Zn is added above about 15 wt. [14].

For Sn, eight out of the 10 points analysed show concentrations below 10 %. Within this subset, no significant differences were observed between unpatinated, patinated exposed and patinated unexposed areas. It is noteworthy that the two points with the highest Sn concentrations coincide with the patinated areas. This observation suggests a surface enrichment of Sn, consistent with the selective leaching phenomenon whereby Cu and Zn corrode more readily than Sn, resulting in surface layers enriched in Sn (Fig. 6B).

Table 1
Elemental compositions of three points of each analysed area: bulk, patina-exposed and patina-not exposed. Values are presented as percentage. n.d.: not detected.

ID	Surface	Mn	Fe	Ni	Cu	Zn	As	Sn	Sb	Pb
Point 1	bulk	n.d.	0.31	0.05	69.17	24.37	n.d.	3.87	0.06	2.21
Point 2	bulk	0,01	0.57	0.26	79.38	9.80	n.d.	7.24	0.09	2.65
Point 3	bulk	n.d.	0.38	0.14	79.25	13.83	n.d.	4.46	0.05	1.92
Point 4	patina - exposed	n.d.	0.65	0.02	69.15	21.69	0.07	4.34	n.d.	4.02
Point 5	patina - exposed	n.d.	0.74	0.01	71.14	20.72	0.02	4.33	n.d.	2.94
Point 6	patina - exposed	0.02	1.47	0.22	75.31	7.90	0.06	11.04	0.09	3.81
Point 7	patina – not exposed	n.d.	1.62	0.01	71.19	19.84	n.d.	3.95	n.d.	3.25
Point 8	patina – not exposed	n.d.	0.81	n.d.	71.39	16.72	n.d.	5.91	n.d.	5.06
Point 9	patina – not exposed	0.02	1.34	n.d.	81.42	0.43	n.d.	14.05	n.d.	2.87
Point 10	patina – not exposed	0.01	1.19	n.d.	71.91	17.03	n.d.	7.05	n.d.	2.77

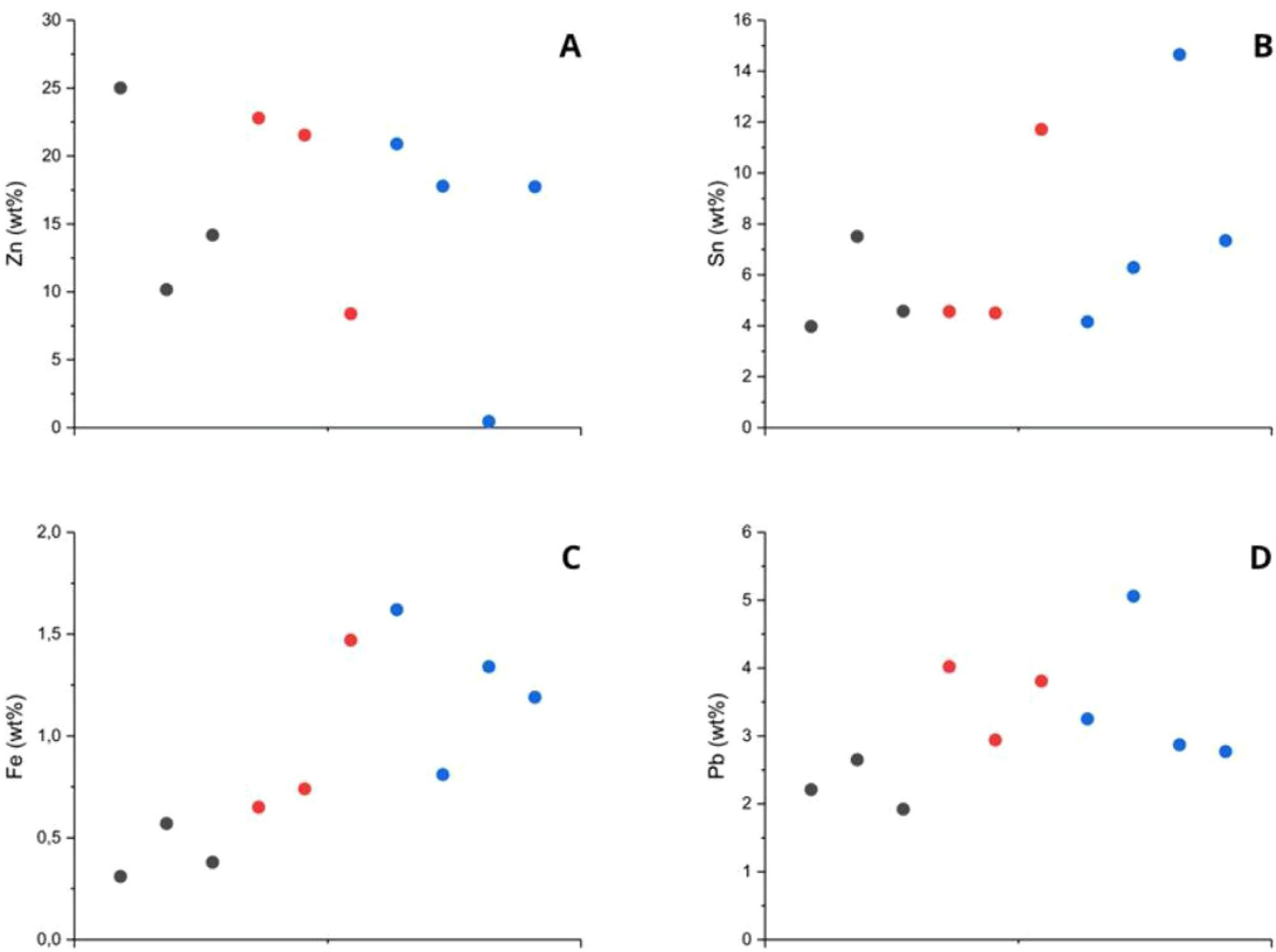

Fig. 6. Plot illustrating (A), Sn (B), Fe (C), and Pb (D) variability across different surface conditions: free-patina areas (black dots), patinated exposed areas (red dots), and patinated non-exposed areas (blue dots). (For interpretation of the references to color in this figure legend, the reader is referred to the web version of this article.)

The potential influence of corrosion, formed because of the statue's interaction with pollutants, moisture, and other environmental factors, is further highlighted by the behaviour of Fe and Pb. Iron content is notably higher in patinated areas, particularly in exposed zones, reaching up to 1.47 % at point 6, which suggests the formation of iron oxides or other corrosion products due to environmental exposure (Fig. 6C). Similarly, Pb is present in higher concentrations in the patinated points (2.87–5.06 %) compared to clearer surfaces (Fig. 6D).

The h-XRF data confirms that the sculpture was produced using a ternary Cu–Sn–Zn alloy rich in lead. The results also highlight the effects of corrosion and weathering on the statue's surface, particularly the zinc depletion and tin enrichment observed in both exposed and unexposed patina areas. These trends are consistent with the typical corrosion behaviour of bronze and brass alloys exposed to atmospheric conditions [15]. The reduction in zinc, especially in the exposed patina, suggests dezincification, a well-known corrosion process in brass where zinc is preferentially leached from the alloy, leaving behind a copper-rich surface more vulnerable to further corrosion [15].

3.3. Composition of the coloured deposits

The heterogeneity of the deposits – often displaying several colour tones - made the portable h-XRF analysis difficult to perform and interpret. Corrosion layers can be composed of the bulk metal ions with lighter elements that are poorly detected when using this type of analysis. The mineralogical composition of the

Table 2
Mineralogical composition of the coloured surface deposits obtained by µ-X-ray diffraction and µ-Raman. The location of the sampling areas is shown in Fig. 4.

Sampling area	Mineral phases	
	µ-XRD	µ-Raman
A	Gypsum (PDF 70-0983), $CaSO_4(H_2O)_2$	Gypsum $CaSO_4(H_2O)_2$;
B	Calcite (PDF47-1743) $CaCO_3$	–
C	Gypsum (PDF 70-0983), $CaSO_4(H_2O)_2$; Cuprite (PDF 05-0667) Cu_2O	Gypsum $CaSO_4(H_2O)_2$;
D	Gypsum (PDF 70-0983), $CaSO_4(H_2O)_2$; Cuprite (PDF 05-0667) Cu_2O	Gypsum, $CaSO_4(H_2O)_2$
E	No displayed pattern	No spectral features
F	No displayed pattern	No spectral features
G	No displayed pattern	Copper phthalocyanine
H	Gypsum (PDF 70-0983), $CaSO_4(H_2O)_2$	No spectral features
I	Hydrated zinc sulphate (PDF 74-1331) $ZnSO_4$ (H2O)/ Gunningite (PDF 01-0621) Hydrated zinc sulphate	No spectral features
J	Gypsum (PDF 70-0983), $CaSO_4(H_2O)_2$	Gypsum $CaSO_4(H_2O)_2$; Chalcantite $CuSO_4{\cdot}5H_2O$
K	Calcite (PDF47-1743) $CaCO_3$	No spectral features

alteration products was evaluated in the laboratory using a µXRD and µRaman and the results are displayed in Table 2. Both µXRD and µRaman showed that most alteration products have gypsum in their composition (Table 2). Raman allowed the identification of gypsum ($CaSO_4(H_2O)_2$) in the surface deposits through the identification of the characteristic bands at 1008 cm^{-1} [1]. One potential origin of $CaSO_4(H_2O)_2$ is the core material within cast statues [17]. During the preparation of a bronze casting mould, the inner core is often filled with a combination of plaster of Paris, water, and sand or clay. Following casting, most of the core material is typically removed but a small fraction remains as a residue. Gypsum deposits can also be a result of wind-carried particles or even an outcome from the reaction of calcium carbonate (calcite, also present in B) with atmospheric or patina-related sulphate ions [17].

Micro-XRD allowed the identification of cuprite (Cu_2O) in two of the collected samples (C and D) and a hydrated zinc sulphate in sampling area I. Complementary analyses were performed with µRaman, but sample fluorescence prevented this complementarity for some of the samples tested. Chalcantite ($CuSO4{\cdot}5H_2O$) was nevertheless identified in one of the samples.

Corrosion represents an irreversible electrochemical process occurring between metals and compounds found in the surrounding environment, ultimately resulting in the modification of the initial metal or alloy composition [5,18]. Zinc from the bulk alloy is being redirected towards the surface and reacting with atmospheric sulphates (from pollution) and water to form a hydrated zinc sulphate. Copper and Zn alloys can suffer from the selective leaching of the later or both metals may dissolve in solution but copper is redeposited on the surface [5]. This process - the removal of Zn - is called dezincification, a process that remains difficult to explain given the complexity of the reactions it encloses [5,15,18]. Regardless, this process depletes the alloy from one of its constituents and this is a situation that requires close monitoring.

Copper phthalocyanine was identified in one sample (G) with spectral features at 1526, 1448, 1340, 744, 678, 480 and 256 nm. This copper salt is used as pigment and corrosion inhibitor and can have a deep blue or a greener shade in the variant of chlorinated copper phthalocyanine [5,19].

VP-SEM-EDS observations of the turquoise-coloured deposits allowed the observation of laminar-shaped crystals (Fig. 7, P2 and P3) and other crystals which appear lighter coloured in BSE (Fig. 7a) due to the presence of Pb (identified by EDS - Fig. 7c). The sampled area appears to be a welding area, where the leg and torso of the statue were joined. The presence of Pb in this area seems to confirm the µXRF results and the use of this metal to join the two parts together.

Both areas showed Cu and Zn, the main constituents of the bulk metal, which suggests that these deposits have their origin in the corrosion of metal or patina. In both cases potassium (K) was de-

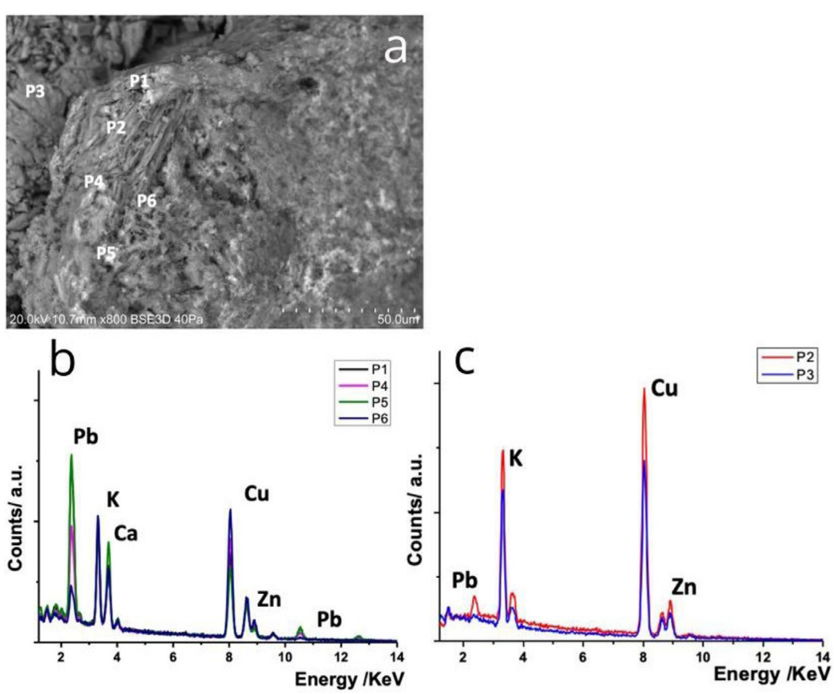

Fig. 7. Turquoise blue deposits accumulated close to a welding area: a) BSE image displaying the selected points for EDS analysis; b) EDS spectra of P1, P4, P5 and P6; c) EDS spectra of P2 and P3. This sample was collected from the location represented in Figs. 2a, 5a and 5a1.

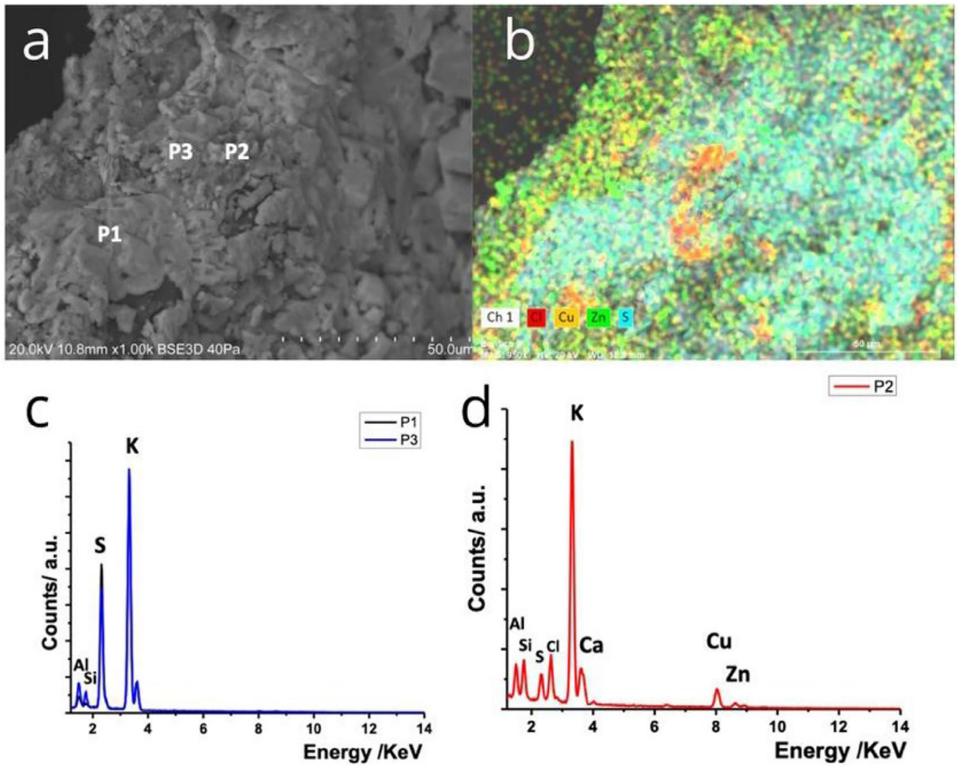

Fig. 8. Turquoise blue deposits: a) BSE image; b) EDS map with Cl, Cu, Zn and S; c) EDS spectra of point P1 and P3; and d) EDS spectra of point P2. (For interpretation of the references to color in this figure legend, the reader is referred to the web version of this article.)

tected but the calcium (Ca) content varied. The possible Ca provenance was explained previously, when discussing XRD results.

Observations of another turquoise-coloured deposit (location E in Fig. 4) under VP-SEM-EDS allowed the observation of different structures (Fig. 8). One of the areas had Cu and Zn, which are the main constituents of the bulk metal reinforcing that some deposits are corrosion products (Fig. 8c and d), being the presence of Chloride (Cl) and Sulphur (S) also detected. Another structure presented no metal, only potassium (K), S, aluminium (Al) and silicon (Si). The presence of K, as in the previous example, might suggest the use of a K-rich compound to produce the dark-coloured patina [20], but could also be present in atmospheric particles.

Observations of the white/orange deposits in location I (right foot, see Fig. 2b and Fig. 4) under SEM allowed the identification of structures with three different compositions (Fig. 9). This is the same location where the presence of hydrated zinc sulphate was determined by µXRD (see Table 1). In one of the points analysed (P1), there were K and S-rich crystals similar to the ones observed in the previous sample. In P2 and P4 the result was rich in Al, Si and K and Cu and Zn were also detected. Finally, a third combination, this one rich in Al, Si, Cl, K and Calcium (Ca), appeared in P3.

The method used to obtain the patina of the statue is unknown. The several elements pinpointed by the SEM-EDS method show a considerable presence of S and K and this is consistent with the use of a sulphur salt of K as there are many patina recipes using salts of sulphur and potassium [20]. As mentioned before, K presence may also be environmental. Lead is present in both the bulk metal and the patina and some patina recipes may also explain the presence of Pb but, again, it is difficult to ascribe them with certainty given the multiplicity of existing recipes and combinations of recipes [20]. As proposed for the gypsum, the Al and Si can come from clay used for the cast, but they can also be environmental contaminants. Chloride was also identified, although in small amounts and this is relevant because green corrosion products such as CuCl (nantokite) and $Cu_2(OH)_3Cl$ (atacamite and polymorphs) can be formed [5,18]. The turquoise-coloured deposits can, in fact, be composed of Cl and Cu, and their presence changes the aesthetic properties of the statue.

Nevertheless, it is important to stress that Cu and Zn were identified with SEM-EDS on the micro fragments of the deposits and this implies that elements from the bulk alloy or patina are emanating from the statue and being deposited on the surface, impoverishing the original composition of the statue. The data collected by the analytical methods applied will educate the conservators so that the best choices (either remedial or preventive, with the application of specific coatings [21]) can be made.

3.4. Mechanical stability of the statue

The technology used offers a wide variety of measurement modes for in situ and non-destructive tests, however, in this particular case, because there is little data on the statue (thickness, manufacture methods) and the fact that it is hollow without access to the interior made it only possible to measure the time that the ultrasounds took to travel through pre-selected areas of the statue, located between the sensors: emitter and receiver. The time measurements (µs, microseconds) were made expediently, placing conductive gel on the segments to be measured and leaning the emitter and receiver against the statue. Fig. 10 presents the obtained results in terms of the time it took for the waves to travel between the emitter and the receiver.

One of the anticipated difficulties of this approach lay on an eventual - and very probable - lack of uniformity in terms of thickness given the casting process used. The other rested on the position of the emitter vs receptor, usually directly opposing each other, a position that was not possible to maintain in this case given the need to circumvent the hollow interior of the statue.

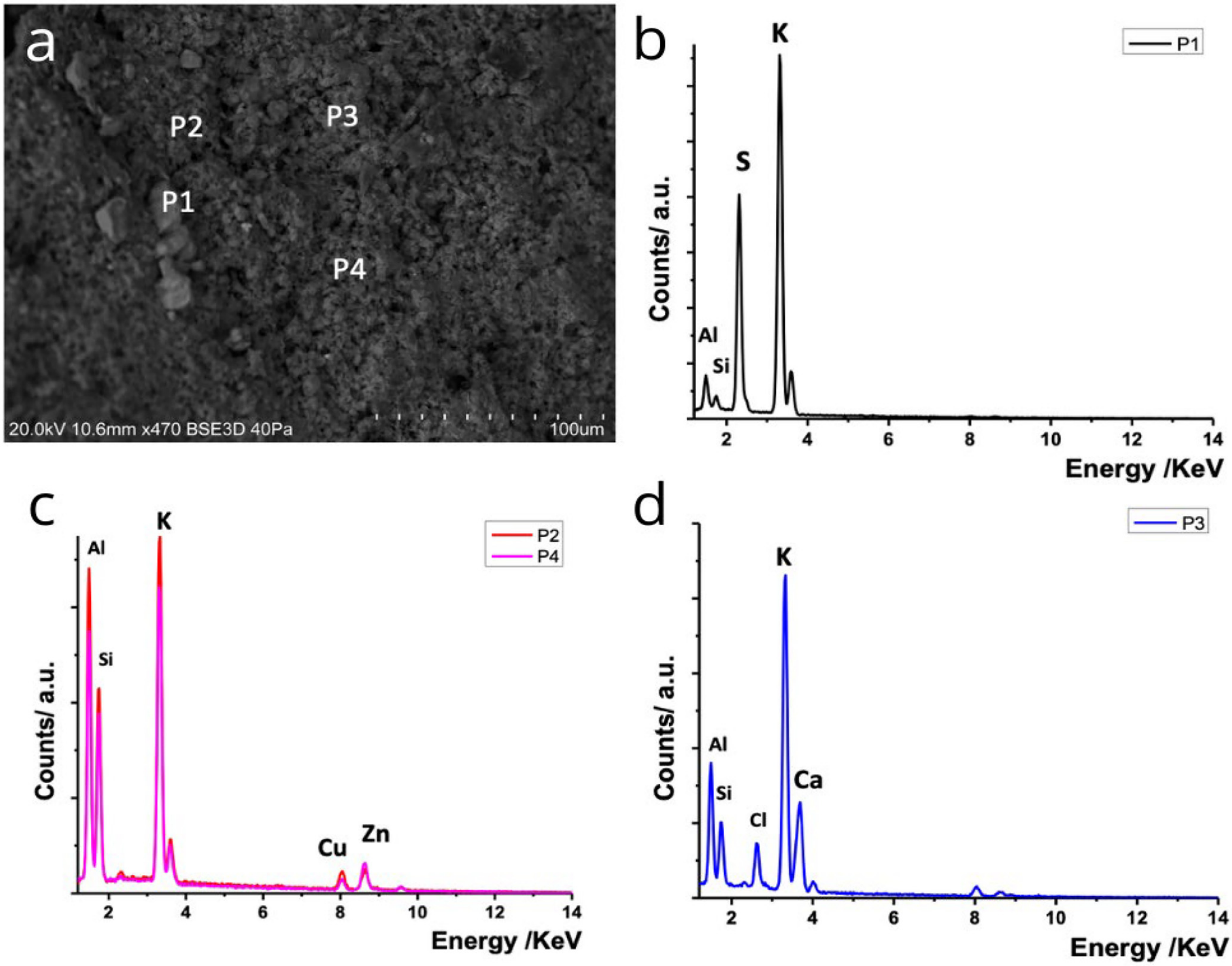

Fig. 9. White/orange deposits: a) BSE image displaying the different points where EDS measurements were performed; b) EDS spectra of point P1; c) EDS spectra of points P2 and P4 and d) EDS spectra of point P3. (For interpretation of the references to color in this figure legend, the reader is referred to the web version of this article.)

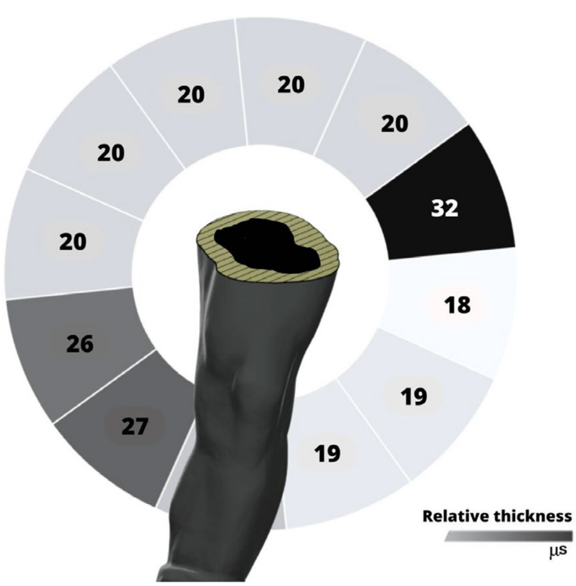

Fig. 10. Thickness results as obtained with the ultrasound technique. The areas where the tone is darker are the thicker ones. The results are consistent with the possible presence of an inner rod in contact with the areas considered thicker.

The results obtained for the leg *thickness* were translated from wave speed and do not correspond to the exact thickness value but do mean that different transmission times were obtained in different areas of the statue leg. This difference indicates that there is a section of the interior and a section of the external area that poses higher resistance to the propagation of the wave. There is, of course, the already mentioned degree of variability in terms of thickness when creating a statue. However, it is also true that if a metallic rod does extend to the upper leg (to sustain the statue as seen in other examples [22]) the locations where this rod is attached to the inner statue may be indicated by the darker regions depicted in Fig. 10. Regardless, there is no way of determining if the condition of this rod is pristine or if the current position of the statue has shifted the internal rod's position and further studies (X-ray radiography and/or boroscopy) [23] are scheduled.

3.5. 3D model

The final 3D can be observed in Figs. 3, 4 and 10. The locations where the alloy composition was determined as well as where samples were taken and studies performed were all demonstrated throughout the article using the 3D Model created. However, creating a 3D model of a metal statue outdoors can be a complex endeavour laden with various challenges [24]. The outdoor environment itself introduces issues such as fluctuating lighting conditions making consistent and detailed captures difficult to acquire. Additionally, weather elements such as rain or wind can distort the statue's surface, affecting the accuracy of scans or photographs used for the model. Public interference can also disrupt the scanning process. The technical obstacles can be equally challenging as metal surfaces pose restrictions due to their reflective nature, causing issues with capturing fine details without unwanted reflections. Complex geometries and intricate designs further complicate the scanning process, potentially creating inaccuracies, particularly when the equipment struggles with capturing elaborate shapes. Moreover, the size of the statue and its location might hinder the ability to capture it entirely. Post-processing of the images acquired under these conditions is a demanding task as texture mapping, especially when original scans lack detailed texture information due to surface reflections, can pose difficulties in accurately depicting the statue's surface.

Overcoming these challenges demands a blend of expertise in 3D scanning, top-notch equipment, suitable environmental conditions, and at times, innovative problem-solving to capture an accurate 3D representation of a metal statue in an outdoor setting. It is, however, a valuable tool to identify, monitor and present the conservation issues [25] the statue is currently facing, as presented in this article.

3.6. Conservation and restoration strategies

The conservation strategies defined by the Storage, Conservation and Restoration Department regarding the Eusébio statue are based on two fundamental principles: the analytical study of the constituent materials and manufacturing processes and the conservation status in order to guarantee both the safety and the preservation of the materiality, aesthetics and artistic values. Within this context, the assessments of the statue's surface provided the team with relevant data, helping define the guidelines for the statue's medium and long-term maintenance.

The surface patina of the statue has a black/dark green coloration, with lighter green areas and golden areas, possibly due to atmospheric exposure and the abrasion of the patina caused by the public's touch and handling.

There are occasional green/blue, and white deposits, most evident in the statue's fine details and pores. These areas are more prone to accumulation of hygroscopic particles, water retention and run-offs, and are therefore more favourable to oxidisation processes of the metal alloy. To stabilise and reduce the degradation processes described the conservation department is mindful of the need to clean the surface of the statue to remove dust, dirt, grease residues from human contact and natural deposits.

The identification of the metal alloy and the characterisation of the oxidation products is fundamental to the definition of the appropriate procedures for the removal and chemical stabilisation of the identified oxidation products. Also, it allowed the selection of the appropriate corrosion inhibitor for copper alloys, as well as the proper definition of a final protective coating with suitable waxes and/or resins, which can act as a physical barrier preventing direct contact with external factors.

Periodic inspections will include re-evaluation of the metallic surface and its evolution (mapping/digital photography) as well as close vigilance on the reappearance of oxidation products.

Regarding structural stability, and as already mentioned, moving and repositioning the statue to its present location may have added mechanical stresses to the left leg that anchors the statue to the ground. These mechanical stresses could accelerate the deterioration of the connection (welding point) between the leg and the torso and be responsible for the alterations visible in Fig. 2a, with accumulation of oxidisation products. Since the statue is outside, accessible to the public, it is essential to evaluate the structural stability and state of conservation of its interior to mitigate the evolution of degradation processes and for obvious safety reasons. The first methodological approach to this pressing issue did not deliver enough conclusions. Further studies are warranted and loading tests, applied at specific points (points that generate the greatest physical deviation from the statue's centre of gravity like the hands and the left foot), with the recording of angle deviation and recovery to the initial position are scheduled. A video endoscopy/boroscopy is also being proposed.

4. Conclusions

The methodologies applied to Eusébio da Silva Ferreira's statue have allowed us to determine the original alloy. Formerly described as bronze, the results revealed instead a tertiary Cu–Sn–Zn alloy rich in Pb due to varying concentrations of these elements that reflect not only differences in alloy composition but may also have been influenced by environmental exposure and corrosion processes over time. In general, the results reveal significant zinc depletion and tin enrichment in the patinated areas, indicative of selective corrosion processes. These findings highlight the importance of considering surface alterations when interpreting the original composition of outdoor bronze statues, as corrosion and weathering can modify surface chemistry. Complementary techniques were necessary for a more in-depth understanding of the metal composition and corrosion behaviour and the information obtained from this study is particularly valuable. It enhances our understanding of the statue's original metallurgical properties and provides insights into the long-term effects of atmospheric conditions on its surface layers.

Analytical techniques have also been proven invaluable in determining the composition of the coloured deposits rendering some of them relatively innocuous while others demand some attention. Atmospheric pollution is potentially responsible for the calcite and gypsum formation. Gypsum can also be secondary to the reaction between calcite and sulphur or even remain from the casting procedure. X-ray diffraction pinpointed the presence of a zinc-hydrated salt, which means a core element of the alloy is being removed and brought to the surface as a corrosion product. Complementing the µXRD results with the SEM-EDS brought to our attention the presence of Zn, Cu and Cl in white and blue deposits, further deepening concerns about active corrosion sites. The chemical profile and associated information are extremely relevant to the conservation approaches being taken by the Storage, Conservation and Restoration Department of Sport Lisboa e Benfica.

Statues that are meant to be touched as a form of homage are a special category of public art. These sculptures are designed to engage the sense of touch, allowing people to physically connect with the subject matter of the statue and pay their respects or express their emotions through this tactile interaction. However, this sort of interaction impacts the conservation and physical stability of the said statue. Therefore, it is essential to be able to conduct a structural assessment and guarantee the safety of these objects and even the public. The ultrasound technique used did not allow us to weave significant considerations on the existence and state of conservation of the stainless-steel rod that supports the statue, and further studies are scheduled to address this pressing issue.

Funding

This work was supported by Portuguese national funds through the FCT—Fundação para a Ciência e a Tecnologia, I.P., within the projects UIDB/04 449/2020 and UIDP/04 449/2020 (HERCULES Laboratory, Évora University), reference LA/P/0132/2020 (IN2PAST—Associate Laboratory for Research and Innovation in

Heritage, Arts, Sustainability and Territory), CEECIND/00,349/2017 (Mathilda Coutinho) and CEECIND/02598/2017 (Ana Catarina Pinheiro). Carlo Bottaini acknowledges UKRI/Marie Curie fellowship (Grant Ref: EP/X020975/1) and FCT project 2022.04844.PTDC (10.54499/2022.04844.PTDC). Marius Araújo acknowledges the European Fund for Regional Development (Interreg/POCTEP) for financing project 0752_MAGALLANES_ICC_5_E.

References

[1] H. Strandberg, Reactions Of Copper Patina Compounds — I. Influence Of Some Air Pollutants, Atmos. Environ. 32 (1998) 3511–3520, doi:10.1016/S1352-2310(98)00057-0.
[2] R.A. Livingston, Acid rain attack on outdoor sculpture in perspective, Atmos. Environ. 146 (2016) 332–345, doi:10.1016/j.atmosenv.2016.08.029.
[3] H. Kwon, N. Cho, Corrosion behaviors of outdoor bronze sculptures in an urban–industrial environment: corrosion experiment on artificial sulfide patina, Metals 13 (2023) 1101, doi:10.3390/met13061101.
[4] H. Kwon, N. Cho, In-situ non destructive investigation of contemporary outdoor bronze sculptures, Herit. Sci. 12 (2024) 1–11, doi:10.1186/s40494-024-01280-8.
[5] D.A. Scott, Copper and Bronze in Art, The Getty Conservation Institute, Los Angeles, 2002.
[6] R.A. Livingston, Influence of the environment on the patina of the statue of liberty, Environ. Sci. Technol. 25 (1991) 1400–1408, doi:10.1021/es00020a006.
[7] Available at: https://www.slbenfica.pt/en-us/instituicao/instalacoes/museu-benfica/patrimonio-cultural/reserva-conservacao-restauro, (n.d.).
[8] M. Sebar, L. Iannucci, L. Grassini, S. Angelini, E. Parvis, M. Antonino, R. Quaranta, G. Giani, C. Boassa, M. Nicola, Corrosion assessment of a bronze equestrian statue exposed to urban environment, KOM – Corros, Mater. Prot. J. 66 (2022) 50–55.
[9] Available at: https://earth.google.com/web/@38.75278345,-9.18488982,81.66582867a,867.24550628d,35y,0h,0t,0r/data=OgMKATA, (n.d.).
[10] I.R. Salta, M. Fontinha, I.R. Salta, M. Fontinha, Diagnóstico Da Corrosão da Estátua de D. José I em Lisboa, Relatório 313/98-NQ, Lisboa, 1998.
[11] European Confederation of Conservator-Restorers'Organisations, E.C.C.O. Professional Guidelines (II) - Code of Ethics, Promoted by the European Confederation of Conservator-Restorers'' Organisations,' (2003). https://www.ecco-eu.org/wp-content/uploads/2021/03/ECCO_professional_guidelines_II.pdf.
[12] T.S. Weisser, The de-alloying of copper alloys, Stud. Conserv. 20 (1975) 207–214, doi:10.1179/sic.1975.s1.035.
[13] P. General-Toro, R. Bordalo, P.R. Moreira, E. Vieira, A. Brunetti, R. Iannaccone, C. Bottaini, Art casting in Portuguese 19th century industrial foundries: a multi-analytical study of an emblematic copper-based alloy monument, Heritage 4 (2021) 3050–3064, doi:10.3390/heritage4040170.
[14] M.L. Young, S. Schnepp, F. Casadio, A. Lins, M. Meighan, J.B. Lambert, D.C. Dunand, Matisse to Picasso: a compositional study of modern bronze sculptures, Anal. Bioanal. Chem. 395 (2009) 171–184, doi:10.1007/s00216-009-2938-y.
[15] M. N. Selvaraj, S. Ponmariappan, S. Natesan, Palaniswamy, Dezincification of brass and its control - an overview, Corros. Rev. 21 (2003) 41–47, doi:10.1515/CORRREV.2003.21.1.41.
[16] M. Maguregui, A. Sarmiento, R. Escribano, I. Martinez-Arkarazo, K. Castro, J.M. Madariaga, Raman spectroscopy after accelerated ageing tests to assess the origin of some decayed products found in real historical bricks affected by urban polluted atmospheres, Anal. Bioanal. Chem. 395 (2009) 2119–2129, doi:10.1007/s00216-009-3153-6.
[17] D. Selwyn, L.S. Binnie, N.E. Poitras, J. Laver, M.E. Downham, Outdoor bronze statues: analysis of metal and surface samples, Stud. Conserv. 41 (1996) 205–228, doi:10.1179/sic.1996.41.4.205.
[18] A. Artesani, F. Di Turo, M. Zucchelli, A. Traviglia, Recent advances in protective coatings for cultural heritage-an overview, Coatings 10 (2020) 217, doi:10.3390/coatings10030217.
[19] P.P. Samal, A. Dekshinamoorthy, S. Arunachalam, S. Vijayaraghavan, S. Krishnamurty, Free base phthalocyanine coating as a superior corrosion inhibitor for copper surfaces: a combined experimental and theoretical study, Colloids Surf. A Physicochem. Eng. Asp. 648 (2022) 129138, doi:10.1016/j.colsurfa.2022.129138.
[20] R. M. Hughes, Rowe, The Colouring, Bronzing and Patination of Metals: a Manual for the Fine Metalworker and Sculptor The Crafts Council, London, 1982.
[21] M.T. Molina, E. Cano, B. Ramírez-Barat, B. Molina, M.T. Cano, E. Ramírez-Barat, Protective coatings for metallic heritage conservation: a review, J. Cult. Herit. 62 (2023) 99–113, doi:10.1016/j.culher.2023.05.019.
[22] G. Bici, M. Campana, F. Colacicchi, O. D'Ercoli, CAD-CAE methods to support restoration and museum exhibition of bronze statues: the "Principe Ellenistico, IOP Conf. Ser. Mater. Sci. Eng. (2018) https://iopscience.iop.org/article/10.1088/1757-899X/364/1/012014.
[23] J. V. Hain, M. Bart, V. Jacko, Use of X-ray microtomography and radiography in cultural heritage testing, In: 11th International Conference on Measurement, 2017.
[24] H.M.C. Nicolae, E. Nocerino, F. Menna, F. Remondino, Photogrammetry applied to problematic artefacts, Int. Arch. Photogramm. Remote Sens. Spatial Inf. Sci. XL-5 (2014) 451–456, doi:10.5194/isprsarchives-XL-5-451-2014.
[25] V.A. Girelli, M.A. Tini, M.G.D. Apuzzo, G. Bitelli, G. Girelli, V.A. Tini, M.A. Apuzzo, M.G.D. Bitelli, 3D Digitisation in cultural heritage knowledge and preservation: the case of the Neptune statue in Bologna and its archetype, in: In the International Archives of the Photogrammetry, Remote Sensing and Spatial Information Sciences, Volume XLI, 2020 XXIV ISPRS Congress (2020 edition), 2020, pp. 1403–1408.